POLITECNICO DI TORINO
Repository ISTITUZIONALE

Multi-fidelity combustion modelling strategy and emission estimation for a hypersonic vehicle powered by air turbo rocket and dual mode ramjet engines

Original
Multi-fidelity combustion modelling strategy and emission estimation for a hypersonic vehicle powered by air turbo rocket and dual mode ramjet engines / Borgna, F., Fusaro, R., Ferretto, D., Saccone, G., Viola, N.. - ELETTRONICO. - (2025), pp. 1-15. (4th International Conference on High-Speed Vehicle Science Technology (HiSST 2025) Tours (Francia) 22-26 September 2025).

Availability:
This version is available at: 11583/3017845 since: 2026-11-12T15:42:29Z

Publisher:
Council of European Aerospace Societies (CEAS)

Published
DOI:

Terms of use:

This article is made available under terms and conditions as specified in the corresponding bibliographic description in the repository

Publisher copyright

(Article begins on next page)

22 November 2026

HiSST: 4th International Conference on
High-Speed Vehicle Science Technology
22 -26 September 2025, Tours, France

Multi-Fidelity Combustion Modelling Strategy and Emission Estimation for a Hypersonic Vehicle Powered by Air Turbo Rocket and Dual Mode Ramjet Engines

F. Borgna[1], R. Fusaro[2], D. Ferretto[3], G. Saccone[4] and N. Viola[5]

Abstract

An advanced multi-fidelity combustion modelling strategy aimed at accurately estimating non-carbon emissions from a hypersonic vehicle is proposed. Specifically, the air-breathing hypersonic case study CS3 (@Mach-5) from the European MORE&LESS project is employed for detailed combustion modelling and subsequent emissions analyses. This vehicle, functioning up to Mach 5.5, is equipped with two distinct air-breathing propulsion systems that operate sequentially during the mission: an Air Turbo Rocket (ATR) for Mach 0–5.5 operations and a Dual Mode Ramjet (DMR) for Mach 4–5.5 operations, both powered by a cryogenic hydrogen feedline. The evaluation of water vapor (H_2O) and nitrogen oxides (NO_x) emissions is conducted for both propulsion systems through the detailed modelling of their combustion processes. The proposed multi-layer modeling approach integrates several simulation strategies to capture the intricate dynamics of combustion under varying operational conditions. Notably, the proposed modelling approaches leverage a single simulation suite, i.e. Cantera, to address the combustion phenomena. The versatility and robustness of Cantera enable simulations that balance incremental improvements in evaluation accuracy with computational complexity and processing time, ensuring that the trade-offs between model fidelity and computational efficiency are optimally managed. For the ATR propulsion system, the combustion process has been investigated using two complementary modelling levels. The first approach analyzes the combustion under the assumption of chemical equilibrium within the combustion chamber, providing steady-state thermodynamic properties and combustion gas compositions. This is complemented by time-dependent chemical-kinetic simulations conducted in a 0D Perfectly Stirred Reactor (PSR) integrated into a preliminary reactor network model, which allows for the evaluation of transient phenomena and a more precise determination of the exhaust gas composition. For the DMR propulsion system, similar modelling strategies have been adopted, with the addition of a refined 1D free flame propagation simulation. This additional layer of analysis enables a deeper insight into the flame dynamics and reaction kinetics that prevail at higher Mach numbers. By systematically comparing the emission outputs from the various modelling layers, the research identifies possible scaling laws among the emission trends at different levels of reliability. Finally, based on the emission results characterized by the highest accuracy, novel low fidelity analytical formulations for NO_x emission indexes estimation are derived. Results indicate that the ATR produces lower NO_x emissions compared to the DMR, in accordance with expectations based on the differing propulsion technologies. Nonetheless, both emission levels remain within acceptable limits for their respective Mach operational ranges. Similarly, the quantity of water vapor released aligns closely with the required combustion efficiency.

[1] *Politecnico di Torino, Corso Duca degli Abruzzi 24, 10129 Turin (Italy), fabrizio.borgna@polito.it*
[2] *Politecnico di Torino, Corso Duca degli Abruzzi 24, 10129 Turin (Italy), roberta.fusaro@polito.it*
[3] *Politecnico di Torino, Corso Duca degli Abruzzi 24, 10129 Turin (Italy), davide.ferretto@polito.it*
[4] *Italian Aerospace Research Centre, Via Maiorise, 81043 Capua (Italy), g.saccone@cira.it*
[5] *Politecnico di Torino, Corso Duca degli Abruzzi 24, 10129 Turin (Italy), nicole.viola@polito.it*

 Copyright © 2025 by author(s)

Keywords: *Combined Air-Breathing Propulsion System; Air Turbo Rocket; Dual Mode Ramjet; Combustion Modelling; 0D/1D Chemical-Kinetic Simulations; Emission Estimation.*

Nomenclature

ATR — Air Turbo Rocket
BFFM2 — Boeing Fuel-Flow Method 2
CRN — Chemical Reactor Network
CS3 — Case Study 3 (MORE&LESS Mach-5 vehicle)
DLR — German Aerospace Center
DMR — Dual Mode Ramjet
EI — Emission Index
ER — Equivalence Ratio
H_2 – molecular hydrogen
H_2O – water vapor (molecular formula)
H2020 — Horizon 2020
ICAO — International Civil Aviation Organization
LTO — Landing–Takeoff cycle
MDO — Multi-Disciplinary Optimization
MFC — Mass Flow Controller / Mass Flow Control law
MORE&LESS — MDO and REgulations for Low-boom and Environmentally Sustainable Supersonic aviation (EU project)
NO — nitric oxide (chemical species)
NO_2 – nitrogen dioxide (chemical species)
NO_x — nitrogen oxides (NO + NO_2, where used collectively)
N_2O – nitrous oxide (chemical species)
P3 — combustor-inlet total pressure
P3-T3 — correlation method employing combustor-inlet total pressure and temperature
PDB — Propulsive Database
PSR — Perfectly Stirred Reactor
STRATOFLY — Stratospheric Flying Opportunities for High-Speed Propulsion Concepts (EU project)
T3 — combustor-inlet total temperature
TRL — Technology Readiness

1. Introduction

The progressive development of hydrogen-fuelled hypersonic propulsion systems presents both technological opportunities and modelling challenges, particularly regarding combustion efficiency and pollutant formation. Hypersonic air-breathing propulsion, particularly when fuelled by hydrogen, represents a promising roadmap for sustainable high-speed transportation and space access. Among the most advanced propulsion architectures under investigation, combined-cycle engines integrating Air Turbo Rockets (ATR) and Dual Mode Ramjets (DMR) offer efficient performance across a wide Mach number range. However, the investigation of combustion processes and pollutant formation mechanisms within such systems remains a complex task due to their operational diversity, high-speed flow regimes, and the strong coupling between chemical kinetics and thermodynamic conditions.
In the context of air-breathing hydrogen combustion, nitrogen oxides (NO_x) formation poses a significant environmental concern. Despite hydrogen's potential for zero-carbon emissions, high flame temperatures and residence times within ATR and DMR chambers promote thermal NO generation via extended Zeldovich pathways [1][2]. Accurate estimation of NO_x emissions under varying flight conditions is thus essential for assessing environmental impact, guiding regulatory compliance, and enabling optimal engine design. Traditional high-fidelity combustion modelling approaches, while capable of capturing detailed kinetics and spatial gradients, are computationally intensive and impractical for iterative system-level analyses. Conversely, overly simplified models often lack the physical fidelity needed to accurately represent emission trends under hypersonic conditions. To bridge this gap, the present study adopts a hierarchical, multi-fidelity modelling strategy that balances accuracy and computational tractability. The proposed framework leverages the Cantera simulation environment [3] and incorporates progressively refined levels of detail, ranging from equilibrium calculations to 0D Perfectly Stirred Reactors (PSRs) and 1D laminar flame simulations. The study focuses on two representative combustion chambers derived from the MORE&LESS (MDO and REgulations for Low-boom and Environmentally Sustainable Supersonic aviation, Grant 101006856) project: the ATR combustor, operating at subsonic to hypersonic Mach numbers, and the DMR combustor, functioning from supersonic to hypersonic speeds. Both are analysed across relevant thermodynamic envelopes

Copyright © 2025 by author(s)

and fuel-air equivalence ratios. Special emphasis is placed on the comparative performance of two chemical kinetic schemes i.e., Z24_NOx20 [4][5] and CRECK_H_O_N [6], selected for their applicability to hydrogen-air mixtures and validated under high-temperature conditions. Beyond emission quantification, a key objective of this work is the derivation of simplified expressions for NO_x emission indices estimation. These compact formulas, grounded in high-fidelity results, are intended for integration into propulsion system simulations and trajectory-level environmental assessments, thereby contributing to the broader objective of designing low-emission, hydrogen-powered hypersonic vehicles. The paper is structured as follows. Section 2 presents the case study (CS3) and introduces the combined-cycle propulsion architecture (Air Turbo Rocket – ATR – and Dual Mode Ramjet – DMR) together with the pre-compiled propulsive database (PDB) and the parametric envelopes selected for the present study. Section 3 details the hierarchical multi-fidelity combustion and emissions methodology: equilibrium calculations, 0D/1D chemical-kinetic simulations and preliminary Chemical Reactor Network (CRN) design. This section documents the chemical-kinetic mechanisms considered and the simulation environment (Cantera). Section 3 also describes the derivation and calibration of compact, semi-empirical NO_x estimation correlations obtained by optimising P3-T3 and BFFM2 exponent coefficients against the medium-fidelity CRN–PSR–Z24 database; the recalibrated correlations enable rapid, low-cost NO_x assessment for system-level and trajectory studies. Section 4 reports numerical results and comparative analyses for the ATR and DMR combustors, including sensitivity of NO_x formation to equivalence ratio, inlet thermodynamic state and modelling choice (PSR vs 1D flame). Key outputs are summarized quantitatively and include $EINO_x$ ranges for the ATR (Z24-based and CRECK-based results), $EINO_x$ behaviour for the DMR across Mach–altitude–ER grids, H_2O production and the optimized analytical formulations for $EINO_x$ estimation. Section 5 draws final conclusions and highlights principal outcomes, practical implications for preliminary design and certification.

2. Case study description

The present work applies a unified emission estimation module to two representative combustor architectures developed within the European H2020 STRATOFLY (Stratospheric Flying Opportunities for High-Speed Propulsion Concepts, Grant 769246) [7] and MORE&LESS [8] research programmes. STRATOFLY sought to demonstrate the technical feasibility of a hypersonic passenger transport flying at altitudes up to 30 km and velocities approaching Mach 8, with the goal of achieving TRL 6 by 2035 while minimising climate impact. Building on STRATOFLY's outcomes, the MORE&LESS project focused on the Mach 5 regime and an optimized environmental footprint, refining both vehicle aerodynamics and propulsion system designs under a holistic, multidisciplinary framework.
Both programmes share a combined Air Turbo Rocket (ATR) + Dual Mode Ramjet (DMR) cycle, but MORE&LESS introduces targeted combustor modifications to suit the reduced enthalpy and pressure levels characteristic of Mach 5 cruise [9].

2.1. ATR Combustor

The Air Turbo Rocket (ATR) combustor is designed for operation during take-off, acceleration, low-to-high-supersonic climb and hypersonic cruise phases (Mach up to ~5.5). The ATR integrates a hydrogen-fuelled gas generator with an air-breathing turbine bypass, offering a compact and throttleable configuration suitable for the initial propulsion phases. Combustion occurs in a subsonic or weakly supersonic flow, with relatively high total temperatures and moderate ignition delay times [10] [11]. Thermodynamic conditions simulated for the ATR combustor are based on parametric modulations of pressure and temperature of the mixture at the inlet of the combustion chamber. The equivalence ratio, with a value close to unity, is assumed to be fixed and constant for all investigated operating conditions. Table 1 summarizes the ranges adopted for these three parameters, which are representative of the engine operating envelope.

 Copyright © 2025 by author(s)

Table 1 ATR operating conditions from pre-compiled propulsive database

	Mach Number [-]	Equivalence Ratio [-]	Mixing Pressure [bar]	Mixing Temperature [K]
MIN	0.3	1.08	0.5	460
MAX	5.5		6.5	1400

These conditions agree with both design points and off-design operating scenarios. NO_x formation is expected to be strongly influenced by flame temperature.

2.2. DMR Combustor

The Dual Mode Ramjet (DMR) combustor operates from Mach ~4 to Mach 5.5, transitioning from ramjet to scramjet mode depending on flight altitude and speed. Combustion takes place under very short residence times and high static temperatures. Operating conditions for the DMR simulation set are summarized in Table 2.

Table 2 DMR operating conditions from pre-compiled propulsive database

	Mach Number [-]	Equivalence Ratio [-]	Mixing Pressure [bar]	Mixing Temperature [K]
MIN	4	0.05	4	850
MAX	5.5	0.8	70	1450

3. Methodology – Combustion simulation and emissions estimation

The combustion modelling and emission estimation strategies adopted in this study are based on a modulated, multi-fidelity approach, designed to balance computational efficiency and physical accuracy across different flow regimes and operating conditions. The proposed layered modelling approach draws from pre-compiled Propulsive Databases (PDBs) and integrates several chemical-kinetic simulations to capture the intricate dynamics of combustion under varying operational conditions. Notably, the proposed modelling approaches leverage a single simulation suite, i.e. Cantera [3], to address the combustion phenomena. The versatility and robustness of the Cantera suite of tools enable simulations that balance incremental improvements in evaluation accuracy with computational complexity and processing time, ensuring that the trade-offs between model fidelity and computational efficiency are optimally managed. The chemical-kinetic emissions estimation module integrates three primary modelling pillars, each based upon the previous in terms of complexity and predictive fidelity, as illustrated by the cascading block diagram in Fig. 1.

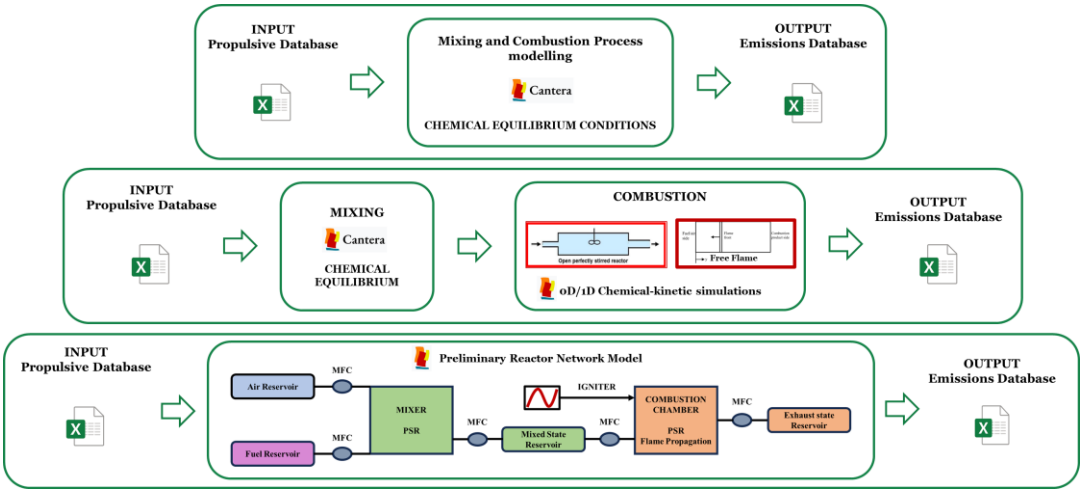


Fig. 1 Combustion simulations - cascading block diagram

Copyright © 2025 by author(s)

1. **Chemical Equilibrium Simulations:** Provides baseline estimates of product composition and flame temperature under the assumption of infinitely fast kinetics and complete mixing. Thermodynamic equilibrium calculations are useful for scoping studies and rapid evaluations across wide parametric modulations but do not account for pollutant specific formation mechanisms, as in the case of NO_x generation sub-mechanisms.
2. **Combustion Chemical-kinetic Simulations:** Zero-dimensional Perfectly Stirred Reactors (PSRs) and one-dimensional freely propagating flame solvers were employed to integrate the species and energy ordinary differential equations under constant pressure and/or volume conditions. Each chemical-kinetic simulation advances until the burned gas temperature equalled the equilibrium flame temperature, ensuring thermodynamic consistency while capturing transient formation pathways of pollutants.
3. **Preliminary Chemical Reactor Network (CRN) models:** Rather than a dense chain of reactors typical of classical CRN approaches, simplified networks composed of a limited number of active (PSR or flame propagator) and passive (reservoir) reactors were interconnected by valve elements with adjustable Mass Flow Control laws (MFC). This structure enabled efficient simulations of primary combustion, intermediate oxidation, and post-combustion zones [12] [13].

For both chemical- kinetic simulations carried out inside individual reactors and when these reactors are embedded within a CRN model, two distinct approximations are proposed to represent the combustion process: (i) combustion of a premixed flow within a zero-dimensional PSR, and (ii) a premixed one-dimensional freely propagating flame. The PSR captures finite-rate chemistry effects by representing the combustor as a well-mixed reactor with prescribed residence time, temperature, and pressure. PSR simulations allow the inclusion of detailed chemical kinetics and are well suited to approximate NO_x formation trends in recirculating zones or in regions where the flame is locally stabilized. The 1D flame provides a higher-fidelity representation of laminar flame structure, thermal gradients, and spatially distributed NO_x production. Although the planar-flame approximation is generally invalid for supersonic combustion, under those conditions a classically propagating flame does not exist because the flame front cannot advance into the unburned mixture owing to the excessively high relative flow velocity, this scenario does not predominate for ATR and DMR engines operating at Mach 5. Consequently, the flame may stabilize as a propagating front and the 1D freely propagating flame approximation can be invoked. The 1D model, therefore, provides important insight into flame thickness, propagation speed, and species stratification that are relevant to the engines' operating envelope. An initial computational verification for this modelling approach, comparing scaled medium-fidelity 0D/1D chemical kinetic simulations (rescaled to approximate 3D conditions) with high-fidelity 3D CFD-LES simulations conducted by the University of Lund, indicates NO mass fractions of the same order of magnitude [14]. Although this inter-model comparison is not equivalent to an experimental validation, it nevertheless strengthens confidence in the multi-level methodology presented here by demonstrating consistency across modelling fidelities under matched boundary conditions.
Each simulation stage is executed using a consistent set of initial conditions, drawn from precompiled PDBs. The flame temperature computed in the first combustion-modelling layer under chemical-equilibrium conditions is used to identify the time at which the time-dependent kinetic–chemical simulations of the two subsequent modelling layers should be terminated. This procedure ensures a unique solution and thermodynamic consistency for each level of the analysis.
Regarding the two more complex modelling layers, the selection of appropriate kinetic mechanisms is a critical element of the analysis. Specifically, the mechanisms chosen must capture, as completely as possible, the formation pathways of nitrogen oxides (NO, NO_2, N_2O), a key combustion product in H_2–air systems alongside H_2O and unburned H_2. Accordingly, three validated hydrogen–air kinetic mechanisms specialized for NO_x prediction were evaluated, and the two most comprehensive mechanisms were selected and employed in the time-dependent simulations. The selected mechanisms offer wide coverage of the relevant temperature and pressure ranges, explicitly represent the important high-temperature reaction pathways (including NO_x formation routes), and have been validated against experimental data reported in the literature:

- **Z22_NOx20**: A reduced mechanism featuring 22 species developed by FOI and tailored for NO formation, offering a balance between accuracy and computational speed [4][5].

 Copyright © 2025 by author(s)

- **Z24_NOx20**: An enhanced extension of the Z22_NOx20 scheme formulated for combustion applications at pressures exceeding 10 bar [4][5].
- **CRECK_H_O_N**: A detailed mechanism developed by the CRECK Modelling Group, comprising hydrogen, oxygen, and nitrogen sub-mechanisms, validated against experimental data in high-pressure, high-temperature hydrogen combustion [6].

The NOx20 sub-mechanism involves not only the thermal Zeldovich NO_x generation reactions but also the interconnected and strongly non-linear reaction paths comprising the HNO and the NH radical chemical routes. Simultaneously, the CRECK_H_O_N has been demonstrated to be the most accurate in the chemical/kinetic assessment of hydrogen combustion in terms of IDT comparison with shock-tube argon diluted measurements in several operative envelopes [5]. Based on the exhaust-gas composition recorded for each simulation, three NO_x emission datasets are built using the Emission Index (EI) parameter, defined as in Eq. 1.

$$EINO_x = 1000 * \frac{Y_{NOx\ outlet\ CC}}{(Y_{H_2\ inlet\ CC} - Y_{H_2\ outlet\ CC})} \left[\frac{g_{NOx}}{kg_{fuel\ burnt}}\right] \quad (1)$$

where Y denotes the mass fractions of NO_x and H_2 at the inlet and outlet of the combustion chamber. These medium-fidelity emissions analyses enable the construction of Emission DataBases (EDBs), which can be employed for subsequent environmental impact assessments and/or recursive optimization of the propulsion concept. Beyond this direct application, the study presents an additional exploitation of the medium-fidelity emissions results: the derivation of low-fidelity analytical tools for rapid emission estimation at virtually zero computational cost. The development of analytical formulations capable of predicting emissions from supersonic-to-hypersonic vehicles fuelled with hydrogen represents a crucial step toward defining sustainability requirements for these vehicle classes from the earliest stages of design, while also providing valuable tools for certification and regulatory processes addressing pollutant and greenhouse-gas emissions. Building upon analytical emission-estimation methods documented in the literature for subsonic aircraft powered by conventional hydrocarbon fuels, a strategy is proposed to extend their applicability to higher-speed regimes and to non-conventional propellants. This strategy leverages medium-fidelity emission data, obtained through chemical-kinetic characterization of the engines, to perform a mathematical optimization of the exponential coefficients in the baseline formulations of the selected estimation methods.

Numerous methodologies exist for the estimation of airborne pollutant and greenhouse-gas emissions. However, for the preliminary assessment of chemical emissions, two compact correlation-based approaches, the P3-T3 method and the Boeing Fuel-Flow Method 2 (BFFM2), represent the most practical compromise between data requirements and predictive fidelity [15]. Correlation-based models can deliver acceptable emission index (EI) estimates but typically demand a large set of input variables, which increases propagated uncertainty [16]. By contrast, P3-T3 and BFFM2 employ a limited parameter set and unified coefficient formulations, thereby enhancing applicability in early design phases. As for NO_x emissions, the P3-T3 formulation corrects sea-level emission indices to flight-level conditions by accounting for combustor-inlet pressure and temperature (P_3, T_3), fuel-to-air ratio and a humidity factor that captures the dampening effect of moisture on NO_x formation. These variables are included in the compact mathematical formulation provided below.

$$\mathrm{EINO_{xFL}} = \mathrm{EINO_{xSL}} \left(\frac{\mathrm{p_{3FL}}}{\mathrm{p_{3SL}}}\right)^{\mathrm{n}} \left(\frac{\mathrm{FAR_{FL}}}{\mathrm{FAR_{SL}}}\right)^{\mathrm{m}} \exp(\mathrm{H}) \quad (2)$$

$$\mathrm{H} = 19 * (\mathrm{h_{SL}} - \mathrm{h_{FL}}) \quad (3)$$

Where H represents the humidity factor, introduced to consider humidity impact on NO_x formation in the combustion chamber. As humidity rises, combustion temperature decreases, reducing NO_x production. The H factor is calculated based on the relative increase in specific humidity h due to altitude gain. Despite not being explicitly included, the combustor inlet temperature T3 implicitly influences the application of the method and serves as a key parameter in the procedure documented in the literature [15]. The generalized formulation typically employs exponent coefficients (n=0.4 and m=0), but optimized coefficients can be used for specific cases to enhance accuracy. The P3-T3 method

Copyright © 2025 by author(s)

is highly versatile and can therefore serve as an excellent tool for estimating NO_x emissions, even in the case of high-speed hydrogen-fuelled aircraft, as documented in the literature [17] for an Air Turbo-Rocket Engine, and [18] for a Synergetic Air-Breathing Rocket Engine concepts using hydrogen. Although it is accurate, its implementation often requires proprietary engine data. Consequently, the fuel-flow methods were derived from P3-T3 to obviate dependence on proprietary inputs by using fuel flow together with ambient pressure, temperature, humidity and Mach number. Among the several fuel-flow methods presented in the literature, the Boeing Fuel-Flow Method 2 (BFFM2) developed by Boeing [19] and its applications [20][21] to sustainable supersonic and hypersonic vehicles [22][18] is considered. The main difference of BFFM2 in comparison to the DLR formulation consist of their exponential correction coefficients. The BFFM2 together with the P3-T3 method are selected for improving owing to their extensive documentation and broad application in the literature. The complete procedure for implementing the original BFFM2 is documented in the literature [19] and includes an additional interpolation step compared to the P3-T3 method.

$$w_{fSL} = w_{fFL} \frac{\theta_{amb}^{a}}{\delta_{amb}^{b}} \exp\left(c * M^{d}\right) \tag{4}$$

$$\theta_{amb} = T_{amb}[K]/288.15 \tag{5}$$

$$\delta_{amb} = p_{amb}[Pa]/101325 \tag{6}$$

$$EINO_{xFL} = EINO_{xSL} \left(\frac{\delta_{amb}^{d}}{\theta_{amb}^{e}}\right)^{f} \exp\left(H\right) \tag{7}$$

where w_f is the fuel flow, H is the humidity factor introduced earlier for the P3-T3 method, and the parameters δ_{amb} and θ_{amb} represent the pressure and temperature ratios of environmental conditions (T_{amb}, p_{amb}) at varying altitudes to those under standard sea level conditions. Similar to the P3-T3 method, it is possible to use exponent coefficients specifically tailored for the engine under study, although the original formulation of the method prescribes the following values: d=1.02, e=3.3, f=0.5. Both P3-T3 and BFFM2 support LTO-cycle assessment, as defined by ICAO [23] via standard thrust settings and can be adapted for hydrogen-fuelled, high-speed propulsion by optimizing exponent coefficients against medium-fidelity, chemistry-resolved emission databases, thus enabling instantaneous emission estimation.

4. Results and Discussion

The numerical simulations highlight distinct NO_x formation behaviours between the ATR and DMR configurations. For the ATR combustor, where flame stabilization occurs under quasi-stagnation conditions with longer residence times, the NO_x emission index exhibits a strong sensitivity to flame temperature. The simulated conditions derive from the pre-compiled PDB; consequently, the engine operating envelope is mapped as follows for the Air Turbo-Rocket. For a prescribed equivalence ratio, a set of candidate flight altitudes is defined and, for each altitude, engine operation is simulated across a range of flight Mach numbers. At each Mach–altitude point the thermodynamic state at the combustor inlet (total temperature and pressure, and derived quantities) is updated and employed as boundary conditions for the combustion models. This mapping generates a multidimensional operating grid that captures the combined effects of altitude, flight speed and inlet thermodynamics on engine performance and emissions.

The spider plots in Figures 2 and 3 depict NO_x Emission-Index (EI) trends obtained with the most advanced modelling layer (preliminary reactor-network models) across a range of flight altitudes and Mach numbers. Figure 2 reports results computed with the Z24_NOx kinetic mechanism, whereas Figure 3 reports results obtained with the CRECK_H_O_N mechanism. The two EI datasets are mutually consistent in terms of order of magnitude and overall profile, although the CRECK_H_O_N scheme systematically yields slightly lower NO_x levels. Trend pattern remains comparable across conditions, with notable divergence at the highest altitudes where the elevated flow regime increases thermochemical loading at the combustor inlet: under these conditions peak flame temperatures occur

 Copyright © 2025 by author(s)

and the differing sub-mechanistic treatments of NO_x chemistry become pronounced. In particular, Z24_NOx is a mechanism highly specialized for NO_x prediction over lean-to-rich mixtures, explicitly resolving both high- and low-temperature NO_x generation pathways with high fidelity; its extensive radical pool and the numerous routes to minor NO_x intermediates consequently produce higher tail-end NO_x predictions in this case compared with those obtained using the CRECK_H_O_N mechanism.
Emission indices for nitric oxide (NO) remain low across the examined Mach–altitude envelope, never exceeding ~50 g·kg^{-1} H_2 when the Z24_NOx mechanism is employed and remaining below ~40 g·kg^{-1} H_2 with the CRECK_H_O_N mechanism, even under worst-case scenarios. Nitrogen dioxide (NO_2) concentrations are effectively negligible and nitrous oxide (N_2O) formation is insignificant for all simulated points. Conversely, water vapour is produced in substantially larger quantities, on the order of 8100 g·kg^{-1} H_2 for both mechanisms, a value that is consistent with the stoichiometry of hydrogen oxidation and with the propulsive performance required by the MORE&LESS CS3 intended mission profile. These results indicate that NO_x emissions from the assessed hydrogen-fuelled high-speed propulsion concepts are confined to relatively low emission-index values within the explored operating envelope, while H_2O production dominates the exhaust composition.

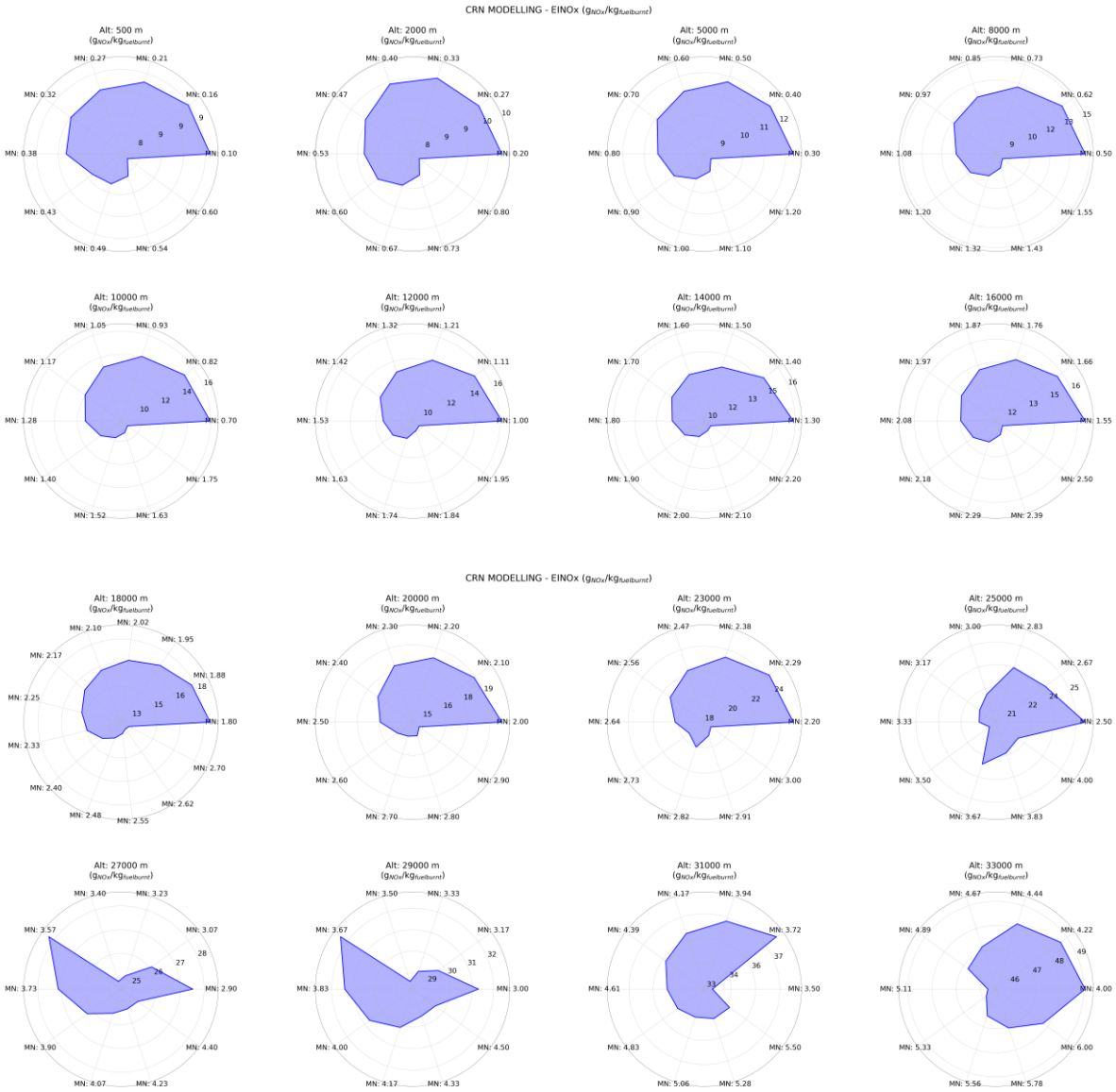


Fig. 2 ATR $EINO_x$ trends obtained with preliminary CRN models (PSR) - Z24_NOx chemical-kinetic mechanism

Copyright © 2025 by author(s)

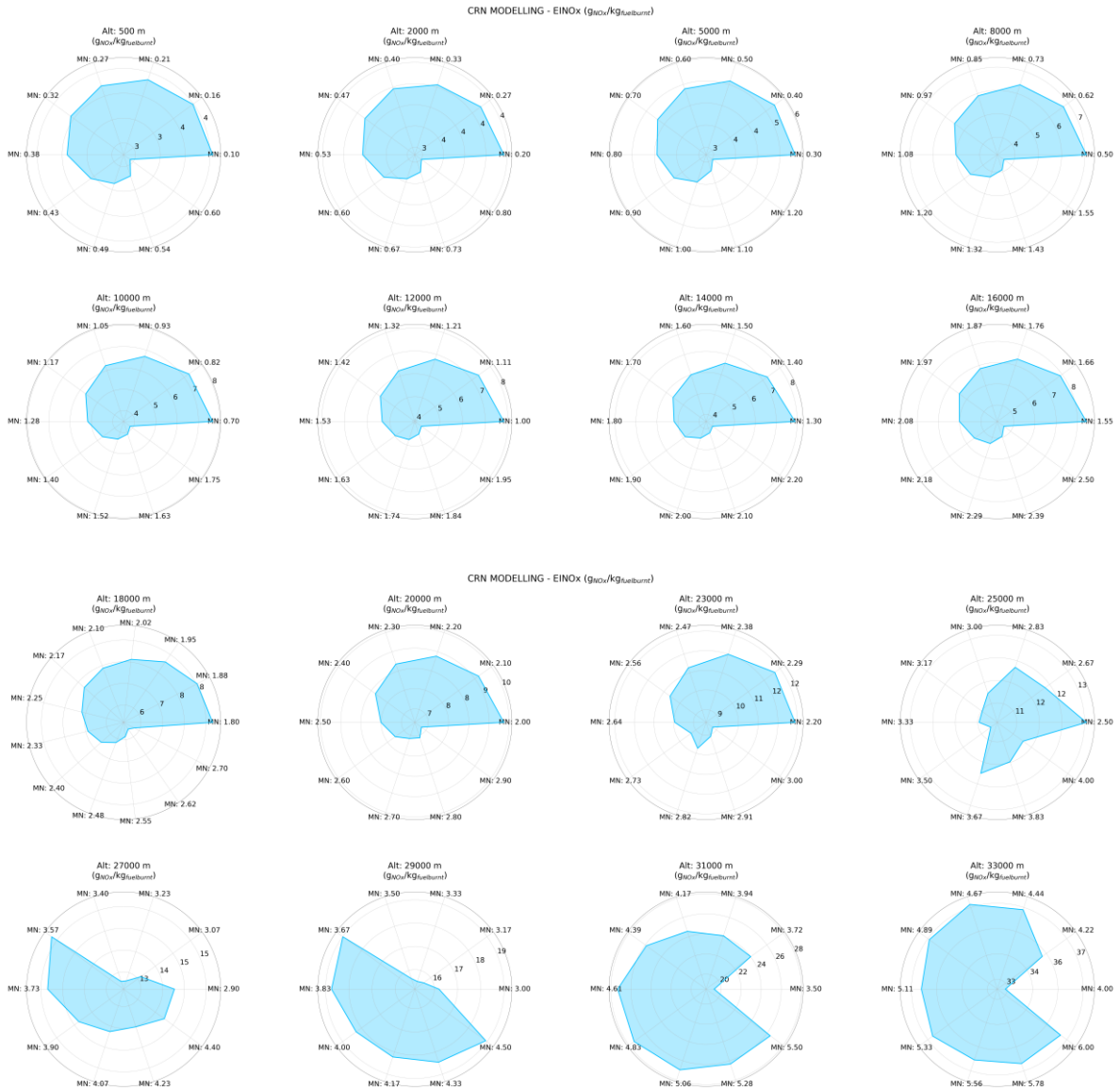


Fig. 3 ATR EINO$_x$ trends obtained with preliminary CRN models (PSR) – CRECK_H_O_N chemical-kinetic mechanism

For the Dual-Mode Ramjet (DMR) the engine operating envelope is mapped by prescribing a discrete set of flight Mach numbers (4.0, 4.25, 4.5, 4.75, 5.0, 5.25 and 5.5), defining candidate flight altitudes for each Mach, and simulating engine operation across a range of equivalence ratios (ER); at each Mach–altitude–ER point the combustor-inlet thermodynamic state is updated and imposed as boundary conditions for the combustion models. Figures 4–7 present NO_x emission-index (EI) trends at the maximum studied Mach number (M = 5.5): results obtained with the Z24_NOx mechanism are reported in Figures 4 and 6, while those obtained with the CRECK_H_O_N mechanism appear in Figures 5 and 7; both Perfectly Stirred Reactor (PSR) and one-dimensional freely propagating-flame (1D flame) modelling are shown (see figure captions). The two kinetic schemes yield mutually consistent EI magnitudes and profiles for lean mixtures, although the CRECK_H_O_N dataset is systematically lower by a modest margin. The 1D freely propagating-flame model substantially underpredicts NO_x relative to PSR results for most high-Mach conditions; this behaviour is attributed to the 1D laminar-flame assumption (steady, one-dimensional propagation) that neglects multi-dimensional effects present at elevated speed e.g., turbulence-induced flame wrinkling, shear and strain rates, shock–boundary-layer interactions, reduced effective residence times, incomplete mixing and recirculation zones, etc. which together limit peak temperature excursions and alter radical pooling compared with realistic combustor

 Copyright © 2025 by author(s)

flow fields [24][25][26]. PSR simulations, by contrast, implicitly represent prolonged residence times and mixed-region chemistry that tend to enhance thermal and prompt NO_x formation. Across the examined Mach–altitude–ER envelope, NO emission indices remain low in most cases ($\lesssim$30 g·kg^{-1} H_2), with isolated peaks approaching ~90 g·kg^{-1} H_2 only at very low ER (combustion-inefficient conditions) where oxidiser limitation and partial oxidation paths promote elevated NO_2 and N_2O formation; under typical operating points NO_2 and N_2O concentrations are effectively negligible. Water vapour production dominates the exhaust composition, on the order of 8700 g·kg^{-1} H_2 for both modelling strategies, consistent with hydrogen-oxidation stoichiometry and the propulsive requirements of the MORE&LESS CS3 mission profile.

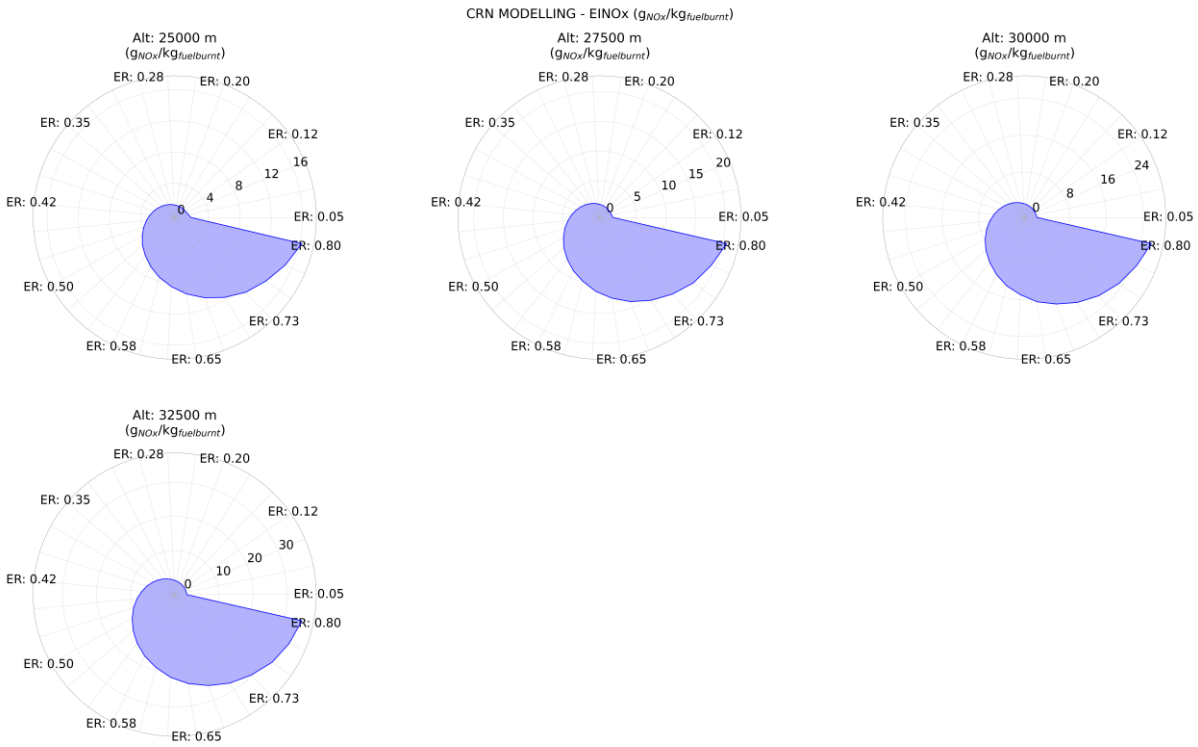


Fig. 4 DMR $EINO_x$ trends obtained with preliminary CRN models (PSR) - Z24_NOx chemical-kinetic mechanism, @Mach5.5

Copyright © 2025 by author(s)

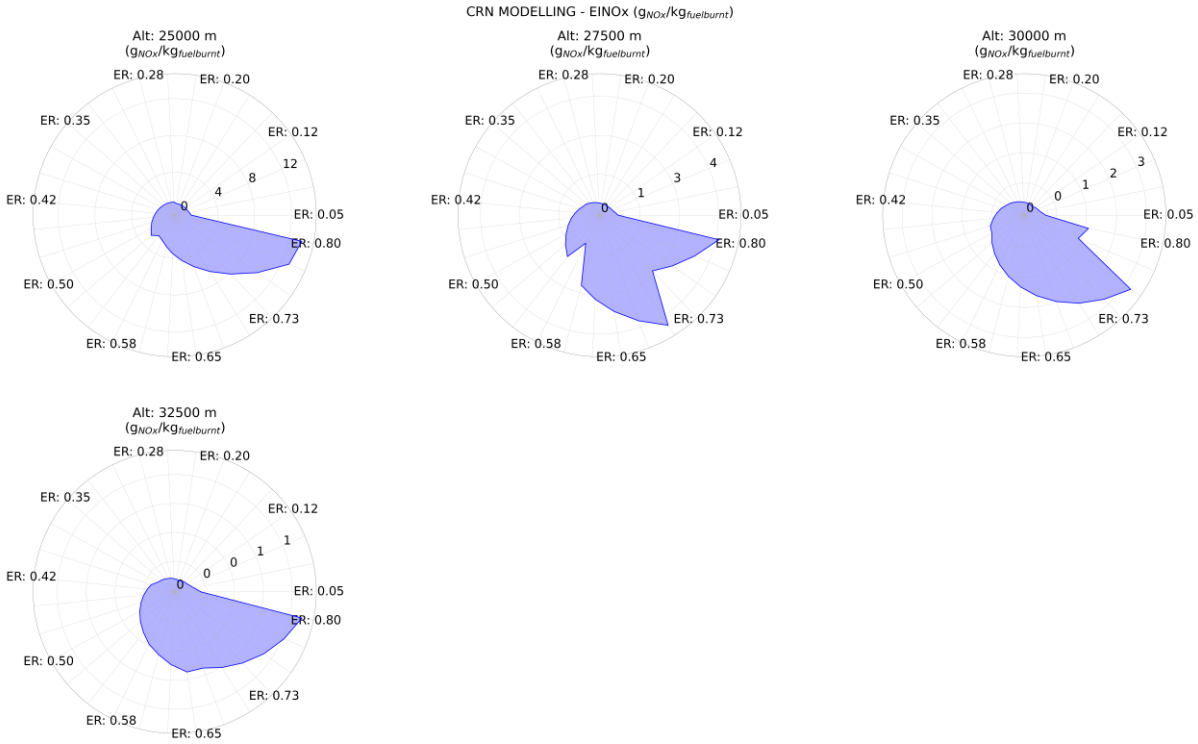


Fig. 5 DMR $EINO_x$ trends obtained with preliminary CRN models (1D free flame) - Z24_NOx chemical-kinetic mechanism, @Mach5.5

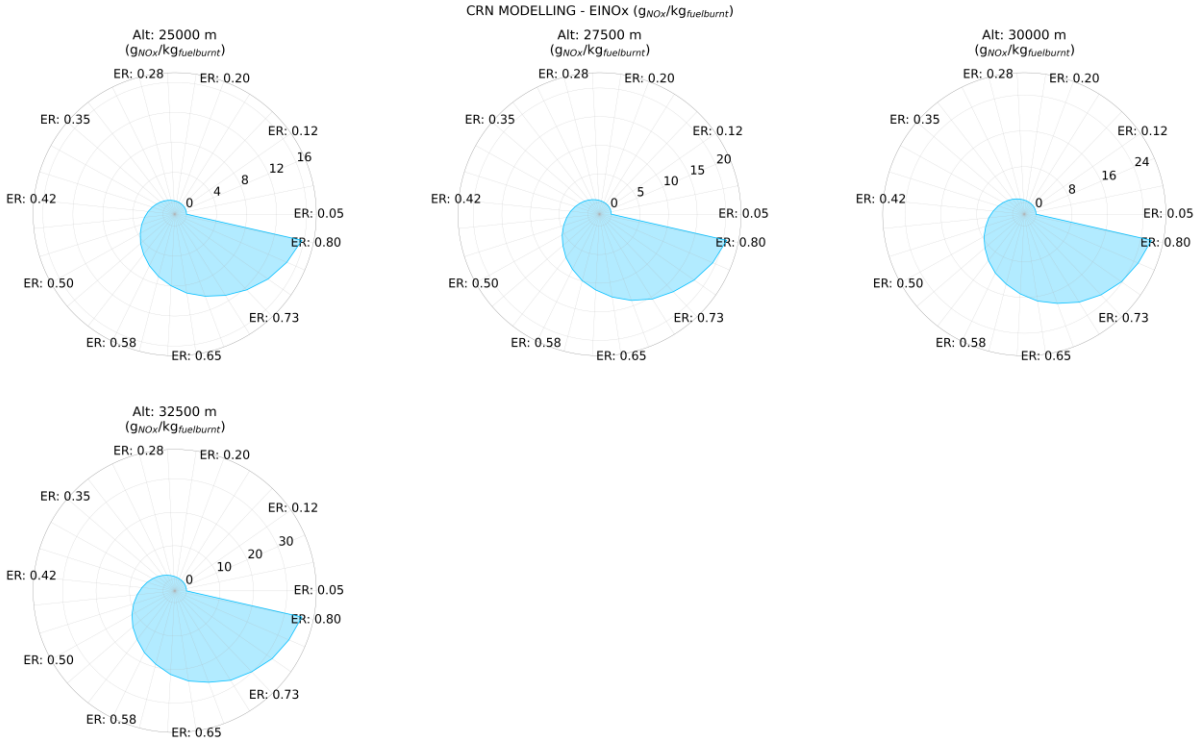


Fig. 6 DMR $EINO_x$ trends obtained with preliminary CRN models (PSR) - CRECK_H_O_N chemical-kinetic mechanism, @Mach5.5

 Copyright © 2025 by author(s)

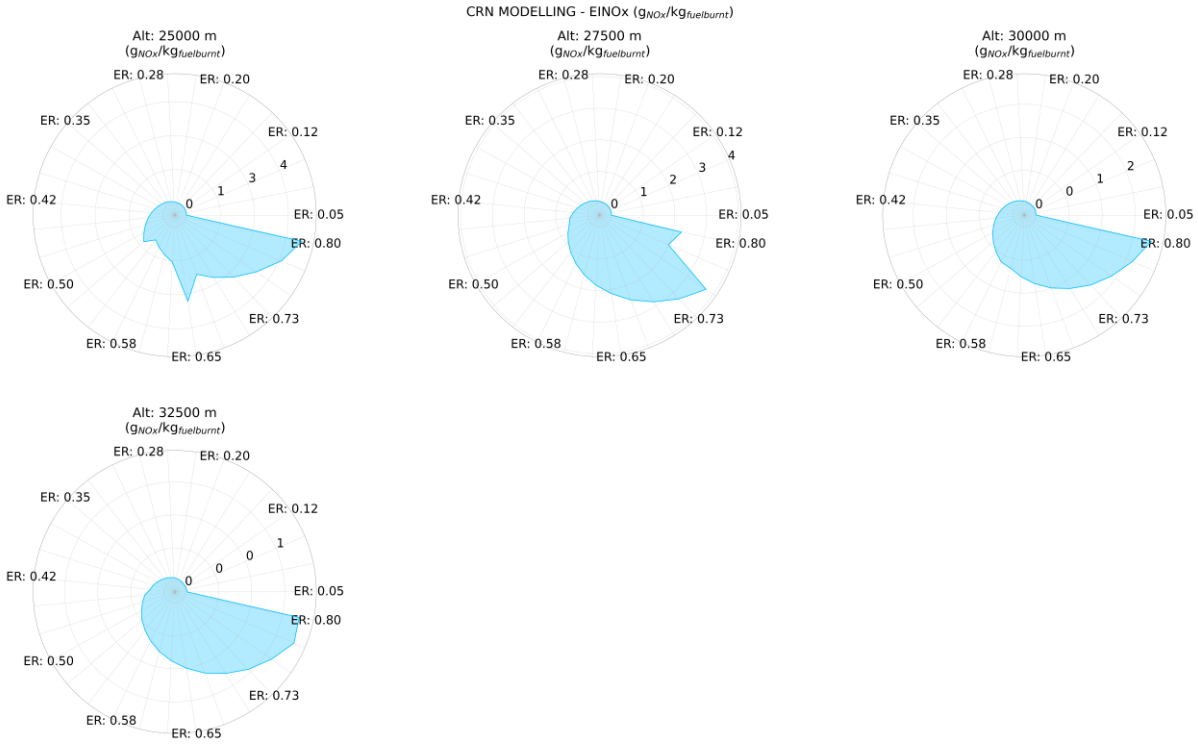


Fig. 7 DMR $EINO_x$ trends obtained with preliminary CRN models (1D free flame) - CRECK_H_O_N chemical-kinetic mechanism, @Mach5.5

Based on the preceding analysis, the combination of the CRN models employing PSR reactor classes together with the Z24_NOx kinetic mechanism is identified as the most conservative configuration for NO_x estimation. The medium-fidelity CRN–PSR–Z24 outcomes are subsequently exploited to derive compact, semi-empirical correlations for instantaneous, low-fidelity prediction of NO_x suitable for system-level models of high-speed vehicles with H_2 fuel. It is observed that the classical unified-coefficient formulations of P3-T3 and BFFM2 systematically overpredict NO_x when exploited beyond subsonic regimes or applied to non-hydrocarbon fuels. Therefore, these baseline formulations are recalibrated. Using a representative sub-dataset extracted from the ATR propulsive and emission databases, the exponential coefficients in the original P3-T3 and BFFM2 expressions are optimized (see Section 3), yielding the updated correlations reported in Equations 8, 9 and 10. Figure 8 illustrates EI trends computed with the original coefficient sets for a limited array of ATR operating conditions, whereas Figure 9 reports the EI trends predicted by the recalibrated formulations against the same reference cases. The recalibration procedure preserves physical-chemical consistency: the numerical values of the updated coefficients are examined and rationalized with respect to the underlying thermochemical correlations governing NO_x formation. Owing to its reliance on combustor-specific inputs, the P3-T3 approach remains intrinsically more accurate than BFFM2 and exhibits a smaller systematic bias; after calibration both updated formulations attain relative errors on the order of unity for the sampled envelope, rendering them practical tools for rapid NO_x assessment in early design and certification workflows.

$$\mathrm{EINO_{xFL}} = \mathrm{EINO_{xSL}} \left(\frac{\mathrm{p_{3FL}}}{\mathrm{p_{3sL}}}\right)^{-0.4} \left(\frac{\mathrm{FAR_{FL}}}{\mathrm{FAR_{sL}}}\right)^{-1.76} \exp(\mathrm{H}) \tag{8}$$

$$\mathrm{w_{fSL}} = \mathrm{w_{fFL}} \frac{\theta_{\mathrm{amb}}^{-3}}{\delta_{\mathrm{amb}}^{-0.16}} \exp\left(0.11 * \mathrm{M}^{-0.41}\right) \tag{9}$$

$$\mathrm{EINO_{xFL}} = 0.6 * \mathrm{EINO_{xSL}} \left(\frac{\delta_{\mathrm{amb}}^{-0.5}}{\theta_{\mathrm{amb}}^{-0.08}}\right)^{0.8} \exp\left(\mathrm{H}\right) \tag{10}$$

Copyright © 2025 by author(s)

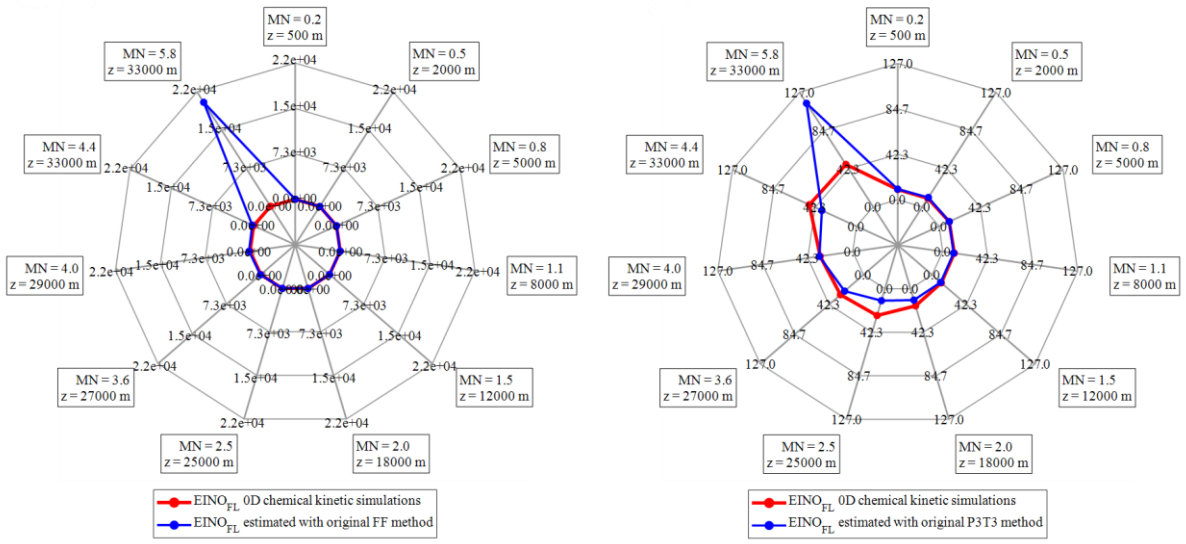


Fig. 8 ATR EINO$_x$ trends obtained with chemical-kinetic simulations vs ATR EINO$_x$ trends obtained with original BFFM2 (left) and P3-T3 (right) methods

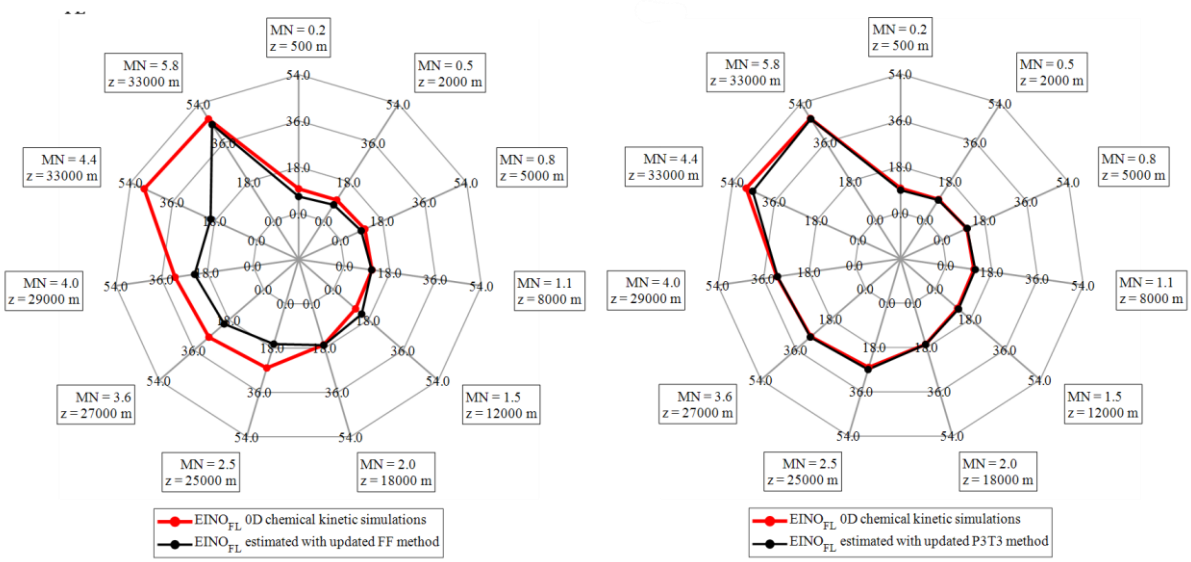


Fig. 9 ATR EINO$_x$ trends obtained with chemical-kinetic simulations vs ATR EINO$_x$ trends obtained with updated BFFM2 (left) and P3-T3 (right) methods

5. Conclusion

A hierarchical multi-fidelity combustion modelling methodology was developed and applied to hydrogen-fueled ATR and DMR combustors of the MORE&LESS CS3 case study. The modelling chain comprises thermodynamic equilibrium calculations, time-dependent 0D PSR integrations and one-dimensional freely-propagating premixed-flame computations embedded within simplified CRNs. All chemical-kinetic simulations were executed with the Cantera environment. Two validated hydrogen–air kinetic schemes were evaluated and the most comprehensive mechanisms selected for transient simulations (Z22/Z24 class and CRECK_H_O_N); these mechanisms explicitly include the main high-temperature NO$_x$ formation pathways, including the extended Zeldovich routes and ancillary H-N–O sub-mechanisms. Quantitative outputs obtained from the medium-fidelity CRN–PSR layer indicate that NO emission

 Copyright © 2025 by author(s)

indices remain low across the examined operating envelopes. For the ATR configuration the Z24-based $EINO_x$ dataset remains $\lesssim 50$ g·kg^{-1} H_2 while the CRECK_H_O_N–based dataset remains $\lesssim 40$ g·kg^{-1} H_2 under worst-case envelope loading. For the DMR configuration typical EI(NO) values are $\lesssim 30$ g·kg^{-1} H_2, with isolated peaks approaching ~90 g·kg^{-1} H_2 occurring only at very low equivalence ratio (extremely lean composition i.e., combustion-inefficient conditions) where incomplete oxidation pathways elevate minor NO_x species (NO_2, N_2O). In all cases NO_2 and N_2O concentrations are negligible for nominal operating points; H_2O production dominates exhaust composition with values on the order of 8.1×10^3–8.7×10^3 g·kg^{-1} H_2, consistent with hydrogen oxidation stoichiometry and the propulsive performance constraints of the mission profile. Outcome comparison demonstrates that the PSR–CRN approach yields systematically higher (more conservative) NO_x estimates relative to the 1D freely-propagating laminar-flame solution at elevated flight speeds. The reduced NO_x predicted by the 1D flame approximation at high Mach arises because the planar laminar-front assumption neglects multi-dimensional flow phenomena. Consequently, the CRN–PSR–Z24 configuration is identified as the most conservative and physically representative model for NO_x estimation in the present context. The medium-fidelity EI datasets were used to recalibrate classical semi-empirical, conceptual design correlation methods (P3-T3 and BFFM2) by optimizing exponential correction coefficients against the CRN–PSR–Z24 database. Recalibration reduces the systematic overprediction observed when the original unified-coefficient formulations are extrapolated to hypersonic regimes or to non-hydrocarbon fuels; the updated correlations reproduce the medium-fidelity EI trends with relative errors on the order of unity across the sampled envelope. The principal deliverables of the study are therefore: (i) accurate emission databases for ATR and DMR engines across the Mach–altitude–ER envelope; (ii) an evidence-based recommendation to adopt CRN–PSR–Z24 as a conservative modelling baseline for NO_x in hydrogen-fueled high-speed propulsion; and (iii) compact, recalibrated P3-T3 / BFFM2 correlations that enable rapid, system-level NO_x assessment with negligible runtime overhead. The low NO_x indices predicted here indicate that hydrogen-fueled air-breathing hypersonic propulsion can be made compatible with stringent emissions goals when combustor thermochemical conditions are controlled; nonetheless, sensitivity to equivalence ratio and off-design operation (particularly for the DMR) is non-negligible and requires further investigation during design and certification. The recalibrated correlations facilitate preliminary environmental assessments, trajectory optimization and regulatory analyses without resorting to computationally expensive kinetic simulations; however, for final certification and to capture localized phenomena (pollutant formation in shear layers, cavity flameholders, etc.) coupling CRN chemistry with spatially-resolved CFD remains recommended. Future work should quantify parametric uncertainty in the correlations, expand the mechanism validation set with additional experimental data at relevant pressure–temperature states, and develop coupled CFD–CRN workflows to resolve multi-dimensional effects identified here.

References

1. Saccone, G., İspir, A. C., Saracoglu, B. H., Cutrone, L., Marini, M.: Computational evaluations of emissions indexes released by the STRATOFLY air-breathing combined propulsive system. *Aircraft Engineering and Aerospace Technology* 94(9), 1499–1507 (2022). [doi:10.1108/AEAT-01-2022-0024]. Emerald
2. Heiser, W. H., Pratt, D. T., Daley, D., Mehta, U. B.: *Hypersonic Airbreathing Propulsion*. AIAA Education Series. American Institute of Aeronautics & Astronautics, Reston, VA (1994). ISBN 978-1-56347-035-6. arc.aiaa.org
3. Goodwin, D. G., Moffat, H. K., Schoegl, I., Speth, R. L., Weber, B. W.: Cantera: An object-oriented software toolkit for chemical kinetics, thermodynamics, and transport processes. Cantera Project, Online, Version 3.1.0 (2024). https://doi.org/10.5281/zenodo.14455267.
4. Zettervall, N.: Reaction mechanism for hydrogen–air combustion. FOI-D-1153-SE. Swedish Defence Research Agency (FOI), Sweden (2022).
5. Saccone, G., Marini, M.: Chemical kinetic analysis of high-pressure hydrogen ignition and combustion toward green aviation. *Aerospace* 11, 112 (2024). https://doi.org/10.3390/aerospace11020112.
6. CRECK Modeling Group: Kinetic-Mechanisms GitHub Repository. Online resource (2023). Available

Copyright © 2025 by author(s)

at: https://github.com/CRECKMODELING/Kinetic-Mechanisms.
7. European Commission — H2020: *Stratospheric Flying Opportunities for High-Speed Propulsion Concepts (STRATOFLY project)*. Grant 769246 (public project pages and outputs). DOI: 10.3030/769246. CORDIS
8. European Commission — H2020: *MDO and REgulations for Low-boom and Environmentally Sustainable Supersonic aviation (MORE&LESS project)*. Grant 101006856. DOI: 10.3030/101006856. CORDIS
9. Viola, N., Fusaro, R., Ferretto, D., Gori, O., Marini, M., Roncioni, P., Cakir, B. O., İspir, A. C., Saracoglu, B. H.: Hypersonic aircraft and mission concept re-design to move from Mach 8 to Mach 5 operations. Proceedings of the 33rd ICAS Congress (ICAS 2022), Stockholm, Sweden; paper ICAS2022_0572, pp. 1–17 (2022). icas.org
10. Fernández-Villace, V., Paniagua, G., Steelant, J.: Installed performance evaluation of an air turbo-rocket expander engine. *Aerospace Science and Technology* 35, 63–79 (2014). SpringerLink
11. Urzay, J.: Supersonic combustion in air-breathing propulsion systems for hypersonic flight. *Annual Review of Fluid Mechanics* 50, 593–627 (2018). https://doi.org/10.1146/annurev-fluid-122316-045217. Annual Reviews
12. Grimm, F.: Low-order reactor-network-based prediction of pollutant emissions applied to FLOX® combustion. *Energies* 15(5), 1740 (2022). https://doi.org/10.3390/en15051740. MDPI
13. Khodayari, H., Ommi, F., Saboohi, Z.: A review on the applications of the chemical reactor network approach on the prediction of pollutant emissions. *Aircraft Engineering and Aerospace Technology* 92(4), 551–570 (2020). doi:10.1108/AEAT-08-2019-0178. DeepDyve
14. Fusaro, R., Piccirillo, G., Ferretto, D., Saccone, G., Bodmer, D., Jäschke, J., Cremaschi, M., Viola, N.: ESATTO: the holistic framework to support the design of sustainable supersonic aviation. Proceedings of the International Council of the Aeronautical Sciences Congress (ICAS 2024); pp. 1–12 (2024).
15. Chandrasekaran, N., Guha, A.: Study of prediction methods for NOx emission from turbofan engines. *Journal of Propulsion and Power* 28, 170–180 (2012).
16. Intergovernmental Panel on Climate Change (IPCC): *Aviation and the Global Atmosphere — Engine Emissions Database and Correlation.* Cambridge University Press (1999).
17. Viola, N., Fusaro, R., Saccone, G., Borio, V.: Analytical formulations for nitrogen oxides emissions estimation of an Air Turbo-Rocket engine using hydrogen. *Aerospace* 10, 909 (2023). https://doi.org/10.3390/aerospace10110909. MDPI
18. Fusaro, R., Borgna, F., Viola, N., Saccone, G.: Analytical formulations for nitrogen oxides emissions estimation of a hydrogen-fueled Synergetic Air-Breathing Rocket Engine (SABRE) in air-breathing mode. *Acta Astronautica* 228, 42–57 (2025). https://doi.org/10.1016/j.actaastro.2024.11.061.
19. DuBois, D., Paynter, G. C.: Fuel Flow Method 2 for estimating aircraft emissions. *SAE Transactions* 115, 1–14 (2006).
20. Dinc, A.: NOx emissions of turbofan powered unmanned aerial vehicle for complete flight cycle. *Chinese Journal of Aeronautics* 33, 1683–1691 (2020). https://doi.org/10.1016/j.cja.2019.12.029.
21. Wang, Y., Yin, H., Zhang, S., Yu, X.: Multi-objective optimization of aircraft design for emission and cost reductions. *Chinese Journal of Aeronautics* 27, 52–58 (2014).
22. Fusaro, R., Viola, N., Galassini, D.: Sustainable supersonic Fuel-Flow Method: An evolution of the Boeing Fuel-Flow Method for supersonic aircraft using Sustainable Aviation Fuels. *Aerospace* 8, 331 (2021).
23. International Civil Aviation Organization (ICAO): *Annex 16 — Volume II: Aircraft Engine Emissions.* ICAO, Montreal (2014).
24. Nair, P. P., Amsha, S., Suryan, A., Nizetic, S.: Investigation of flow characteristics in supersonic combustion ramjet combustor toward improvement of combustion efficiency. *International Journal of Energy Research* 45, 231–253 (2021). https://doi.org/10.1002/er.5257.
25. Thillai, N., Thakur, A., Srikrishnateja, K., Dharani, J.: Analysis of flow-field in a dual mode ramjet combustor with boundary layer bleed in isolator. *Propulsion and Power Research* 10(1), 37–47 (2021). https://doi.org/10.1016/j.jppr.2020.10.004.
26. Cooper, M., Sam, A. A., Pesyridis, A.: Modelling of a dual-fuel-mode free-jet combustion system. *Aerospace* 6(12), 135 (2019). https://doi.org/10.3390/aerospace6120135.

 Copyright © 2025 by author(s)